PHYSICAL REVIEW B **95**, 241303(R) (2017)

Exchange-only singlet-only spin qubit

Arnau Sala and Jeroen Danon
Department of Physics, NTNU, Norwegian University of Science and Technology, 7491 Trondheim, Norway
(Received 9 February 2017; revised manuscript received 29 May 2017; published 19 June 2017)

We propose a feasible and scalable quantum-dot-based implementation of a singlet-only spin qubit which is to leading order intrinsically insensitive to random effective magnetic fields set up by fluctuating nuclear spins in the host semiconductor. Our proposal thus removes an important obstacle for further improvement of spin qubits hosted in high-quality III-V semiconductors such as GaAs. We show how the resulting qubit could be initialized, manipulated, and read out by electrical means only, in a way very similar to a triple-dot exchange-only spin qubit. Due to the intrinsic elimination of the effective nuclear fields from the qubit Hamiltonian, we find an improvement of the dephasing time T_2^* of several orders of magnitude as compared to similar existing spin qubits.

DOI: 10.1103/PhysRevB.95.241303

Spin qubits in semiconductor quantum dots are one of the more promising scalable qubit implementations put forward so far [1]. The original proposal almost two decades ago [2] was rapidly followed by early experimental successes, including demonstration of the principles of qubit initialization, manipulation, and readout [3,4]. At the same time, two main challenges for further progress were identified: (i) Single-qubit manipulation requires highly localized oscillating magnetic fields, which are very hard to realize in practice. (ii) All high-quality III-V semiconductors (such as GaAs) consist of atoms carrying nonzero nuclear spin, and the fluctuating ensemble of nuclear spins in each quantum dot couples to the spin of localized electrons through a hyperfine interaction. This coupling causes spin relaxation [5] and yields random effective local magnetic fields acting on the electron spins, which present an important source of qubit decoherence [6,7]. Most of the work in the field of semiconductor spin qubits in the past decades has been aimed at overcoming these two challenges.

One proposed way to overcome the requirement of oscillating magnetic fields is to use a material with a relatively strong spin-orbit interaction (such as InAs), in which coherent spin rotations could be achieved by the application of oscillating *electric* fields [8–10]. A drawback is that the spin-orbit interaction contributes to qubit relaxation [11] and also interferes with the spin-to-charge conversion commonly used for qubit initialization and readout [12]. Another approach is to encode the qubit in a *multielectron* spin state, which enables qubit control through (gate-tunable) exchange interactions [13]: Using two-electron spin states in a double quantum dot, one can define a qubit in the unpolarized singlet-triplet (S-T_0) subspace, which allows for electrical control of qubit rotations along one axis of the Bloch sphere [14,15]; recently it was realized that with one more quantum dot (and electron) one can use two three-electron spin states to define a qubit that has *two* such control axes [16]. The resulting triple-dot exchange-only (XO) qubit can thus be fully operated by electrical means only [16–18]. The downside of using exchange-operated spin qubits is their increased sensitivity to charge noise, either coming from environmental charge fluctuations or directly from the gates. However, recent work indicates that symmetric operation of such qubits could greatly reduce their sensitivity to charge noise [19–21].

These successes thus eliminated the need for highly localized oscillating magnetic fields, leaving the problem of the nuclear spins as the main intrinsic obstacle for further progress [22–25]. Common approaches to overcome this problem include devising hyperfine-induced feedback cycles, where driving the electronic spins out of equilibrium results in a suppression of the fluctuations of the nuclear spin ensemble [26–30], as well as optimizing complex echo pulsing schemes, where the dominating frequencies in the spectrum of the nuclear spin fluctuations are effectively filtered out [31–33], or via a Hamiltonian parameter estimation to operate the qubit with precise knowledge of the environment [34]. Although some of these ideas led to significantly prolonged coherence times, they all involve a large cost in overhead for qubit operation. Another promising approach is to host spin qubits in isotopically purified silicon, which can be (nearly) nuclear spin free [35–37], but the stronger charge noise and the extra valley degree of freedom complicate their operation.

Here, we propose a type of spin qubit that can be hosted in GaAs-based quantum dots, but (i) is intrinsically insensitive to the nuclear fields in the dots and (ii) can be operated fully electrically, similar to the triple-dot XO qubit. The idea is to encode the qubit in a *singlet-only* subspace, which is known to be "decoherence free" for spin qubits (in the sense that fluctuating Zeeman fields do not act inside the subspace) [38,39]. It turns out that a system of four spin-$\frac{1}{2}$ particles hosts such a subspace [40,41]: Among the 16 different four-particle spin states there are two singlets, thus providing a decoherence-free two-level subspace. Below, we present a feasible implementation of a qubit in this subspace, using four electrons in a quadruple quantum dot. We include a clearly outlined scheme for initialization, manipulation, and readout of this qubit, as well as an investigation of its performance in realistic circumstances. We find that, at the price of a slight increase in complexity beyond the triple-dot XO setup, our qubit has superior coherence properties, extending T_2^* by orders of magnitude, while still having a highly scalable design.

The qubit. We propose a setup in which four quantum dots are arranged in a T-like geometry, as shown in Fig. 1(a), where solid lines connect dots that are tunnel coupled. Nearby charge sensors, indicated by "M", can be used to monitor the charge state (N_1,N_2,N_3,N_4) of the quadruple dot, where N_i is

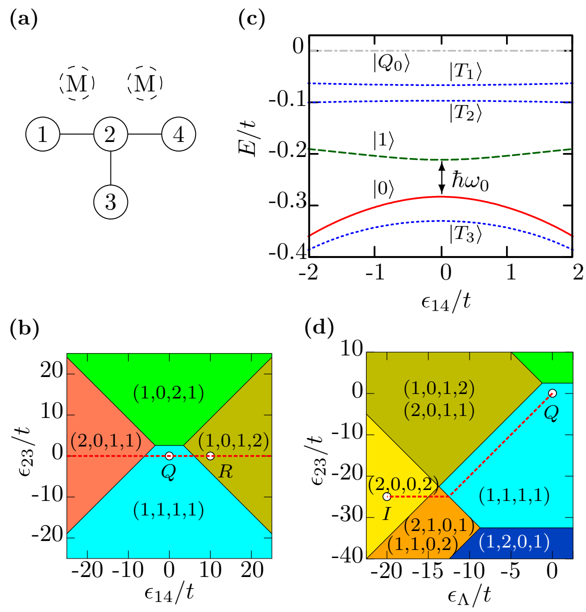

FIG. 1. (a) Schematic representation of the quadruple-dot geometry. The four dots are labeled 1–4 and solid lines indicate which dots are tunnel coupled. The dashed circles labeled "M" show suggested positions for charge sensors. (b) Charge stability diagram in the four-electron regime as a function of ϵ_{14} and ϵ_{23}, using $U = 50t$, $U_c = 15t$, and $\epsilon_\Lambda = 0$. The red dashed line shows the tuning axis along which the qubit is operated. (c) Spectrum of the subspace with $S_z = 0$ along the red dashed line in (b), with $t_{12} = t_{24} = \frac{4}{3}t_{23} = t$. Only the lowest part of the spectrum is shown. The red solid and green dashed lines correspond to the two singlet states that form the qubit. (d) Charge stability diagram as a function of ϵ_Λ and ϵ_{23} with $\epsilon_{14} = 0$ and further the same parameters as in (b). The red dashed line shows the path we suggest for qubit initialization.

the number of excess electrons on dot number i, as labeled in Fig. 1 [42]. To describe this system, we use a Hubbard-like Hamiltonian [43,44],

$$\hat{H} = \sum_i \left[\frac{U}{2}\hat{n}_i(\hat{n}_i - 1) - V_i\,\hat{n}_i\right] + \sum_{\langle i,j\rangle} U_c\,\hat{n}_i\hat{n}_j - \sum_{\langle i,j\rangle,\alpha} \frac{t_{ij}}{\sqrt{2}}\,\hat{c}^\dagger_{i,\alpha}\hat{c}_{j,\alpha} + \sum_{i,\alpha}\frac{E_Z}{2}\,\hat{c}^\dagger_{i,\alpha}\sigma^z_{\alpha\alpha}\hat{c}_{i,\alpha}, \tag{1}$$

where $\hat{n}_i = \sum_\alpha \hat{c}^\dagger_{i,\alpha}\hat{c}_{i,\alpha}$ with $\hat{c}^\dagger_{i,\alpha}$ the creation operator for an electron with spin α on dot i. The first line of Eq. (1) describes the electrostatic energy of the system: The first term accounts for the on-site Coulomb interaction of two electrons occupying the same dot, the second term adds a local offset of the potential energy that can be controlled via gating, and the last term describes the cross capacitance between neighboring dots. To this we added (spin-conserving) tunnel couplings between neighboring dots, characterized by coupling energies t_{ij}, and a uniform Zeeman splitting of the electronic spin states induced by an external magnetic field applied along the z direction, where $E_Z = g\mu_B B$ is the Zeeman energy, with g the effective g factor ($g \approx -0.4$ in GaAs), μ_B the Bohr magneton, and B the magnitude of the applied field.

We can use the electrostatic part of $\hat{H}$ to find the charge ground state as a function of the gate-induced offsets V_i. For convenience, we introduce the tuning parameters $\epsilon_{14} = (V_4 - V_1)/2$, $\epsilon_{23} = (V_3 - V_2)/2$, $\epsilon_\Lambda = (-V_1 + V_2 + V_3 - V_4)/4$, and $\epsilon_\Sigma = (V_1 + V_2 + V_3 + V_4)/4$, where we fix $\epsilon_\Sigma = \frac{3}{4}U_c$. Focusing on the four-electron regime, we show a part of the resulting charge stability diagram as a function of ϵ_{14} and ϵ_{23} in Fig. 1(b), where we have set $\epsilon_\Lambda = 0$, $U = 50t$, and $U_c = 15t$ (t being our unit of energy, of the order of the tunnel coupling energies). Our region of interest is the "top" of the (1,1,1,1) charge region, where exchange effects due to the vicinity of the (2,0,1,1), (1,0,2,1), and (1,0,1,2) charge regions can be significant and are effectively tunable through the gate potentials V_i. We note here that we will assume throughout that the orbital level splitting on the dots is the largest energy scale in the system (larger than U), so we will only include states involving double occupation ($N_i = 2$) if the two electrons are in a singlet state.

We now include finite tunnel coupling energies t_{ij} and a Zeeman energy E_Z, and investigate the spectrum of $\hat{H}$ in more detail. The red dashed line in Fig. 1(b) indicates where $\epsilon_{23} = 0$, and along this line ϵ_{14} parametrizes a "linear tilt" of the potential of the three dots 1, 2, and 4, equivalent to the triple-dot detuning parameter that is used to operate the XO qubit (see Refs. [16,23,44]). In Fig. 1(c) we plot the resulting spectrum of the six lowest-lying states with $S_z = 0$ along this line, as a function of ϵ_{14}, where we have set $t_{12} = t_{24} = \frac{4}{3}t_{23} = t$ and $E_Z = 1.875t$. In the plot we can identify one quintuplet state $|Q_0\rangle$ (gray dotted dashed), three triplet states $|T_{1,2,3}\rangle$ (blue dotted), and two singlets (green dashed and red solid). The ten other spin states, having $S_z = \pm1, \pm2$, are split off by multiples of E_Z and not shown in the plot.

The two singlets we propose to use as qubit basis states are marked $|0\rangle$ and $|1\rangle$ in Fig. 1(c) and read to lowest (zeroth) order in the tunnel couplings t_{ij}

$$|1\rangle = |S_{14}S_{23}\rangle, \tag{2}$$

$$|0\rangle = \frac{1}{\sqrt{3}}\{|S_{13}S_{24}\rangle + |S_{12}S_{34}\rangle\}, \tag{3}$$

where S_{ij} denotes a singlet pairing of the two electrons in dots i and j. As an example, one can write explicitly $|1\rangle = \{|\uparrow\uparrow\downarrow\downarrow\rangle - |\uparrow\downarrow\uparrow\downarrow\rangle - |\downarrow\uparrow\downarrow\uparrow\rangle + |\downarrow\downarrow\uparrow\uparrow\rangle\}/2$.

Close to the central point $\epsilon_{14} = 0$, marked Q in Fig. 1(b), exchange effects are small in t/Δ, where $\Delta = U - 3U_c$ is the half width of the (1,1,1,1) charge region along the detuning axis ϵ_{14}, and we thus treat the tunnel couplings as perturbations. Including only the nearby charge states (2,0,1,1), (1,0,2,1), and (1,0,1,2), we can project $\hat{H}$ to the qubit subspace spanned by $|0\rangle$ and $|1\rangle$, yielding to second order in the t_{ij},

$$\hat{H}_{\rm qb} = \frac{1}{4}(J_{12} + J_{24} - 2J_{23})\hat{\sigma}^z + \frac{\sqrt{3}}{4}(J_{12} - J_{24})\hat{\sigma}^x, \tag{4}$$

where we subtracted a constant offset. The $\hat{\sigma}^{x,z}$ denote Pauli matrices, and the relative magnitudes of the exchange energies $J_{12} = t_{12}^2/(\Delta + \epsilon_{14})$, $J_{24} = t_{24}^2/(\Delta - \epsilon_{14})$, and $J_{23} = t_{23}^2/\Delta$, can be controlled by the detuning parameter ϵ_{14} (note that we have set $\epsilon_{23} = 0$). We make two observations: (i) The qubit splitting at zero detuning, $\hbar\omega_0 = (t_{12}^2 + t_{24}^2 - 2t_{23}^2)/2\Delta$, vanishes if all three tunnel couplings are equal; ideally, one tunes $t_{12} = t_{24} \neq t_{23}$. (ii) The structure of this Hamiltonian is fully equivalent to that of the triple-dot XO qubit [cf. Eq. (5) in Ref. [44]], including its qualitative dependence on the detuning parameter. Thus, our qubit can be operated analogously to the XO qubit, i.e., by static pulsing [16] or resonant driving [23], and the point Q is a sweet spot where the qubit is to lowest order insensitive to noise in ϵ_{14}.

Qubit operation. Qubit rotations are most conveniently achieved using resonantly driven Rabi oscillations [23]. For small detuning, $|\epsilon_{14}| \ll \Delta$, we can expand $\hat{H}_{\rm qb}$ to linear order in ϵ_{14}, yielding

$$\hat{H}_{\rm qb} = \frac{1}{2}\hbar\omega_0\hat{\sigma}^z - \frac{\sqrt{3}}{2}\frac{t^2\epsilon_{14}}{\Delta^2}\hat{\sigma}^x, \tag{5}$$

where we used $t_{12} = t_{24} = t$. A harmonic modulation of the detuning, $\epsilon_{14} = A\cos(\omega\tau)$, will thus induce Rabi rotations of the qubit which will have at the resonance condition $\omega = \omega_0$ a Rabi period of $T_{\rm Rabi} = 4\pi\hbar\Delta^2/(\sqrt{3}t^2A)$. Using again $\Delta = 5t$ (consistent with the realistic parameters $t = 20$ μeV, $U = 1$ meV, and $U_c = 0.3$ meV), a moderate driving amplitude of $A = 2.5$ μeV would yield a rotation time $T_{\rm Rabi} \approx 50$ ns.

Readout of the qubit can be performed by spin-to-charge conversion, in a similar way as in the double-dot S-T_0 [14] and triple-dot XO [16,23] qubits. The detuning ϵ_{14} is quickly pulsed to the point marked R in Fig. 1(c), which lies in the (1,0,1,2) charge region. There are only two accessible (1,0,1,2) states with $S_z = 0$: The two electrons on dot 4 must be in a singlet state, but the electrons on dots 1 and 3 can form either a singlet S or unpolarized triplet T_0. Only the singlet-singlet configuration couples adiabatically to one of the qubit states (the state $|0\rangle$). After pulsing to R, the qubit state $|0\rangle$ will thus transition to a (1,0,1,2) charge configuration whereas the state $|1\rangle$ remains in a spin-blockaded (1,1,1,1) state. Subsequent charge sensing amounts to a projective measurement of the qubit state. One requirement is that the detuning pulse has to be fast enough so that spin-flip transitions from $|0\rangle$ to one of the lower-lying states with $S_z = 1,2$, which are crossed at $\epsilon_{14} \sim E_Z$, are very unlikely. (Note that exactly the same condition holds for the triple-dot XO qubit measurement scheme, where the spin-$\frac{1}{2}$ state connected to $|0\rangle$ crosses a spin-$\frac{3}{2}$ state [23].)

Initialization of the qubit can be achieved in a similar way. The simplest procedure is to pulse to a point in gate space where there is one unique singlet-only ground state, such as the point marked I in the (2,0,0,2) charge region [see Fig. 1(d)]. After waiting long enough, the system will have relaxed to this ground state, and a fast pulse back to the qubit tuning Q will yield a qubit prepared in $|0\rangle$. The path we propose for this pulse is marked in Fig. 1(d) by a red dashed line: First, ϵ_Λ is increased until the edge of the (1,1,1,1) charge region is reached, after which both ϵ_Λ and ϵ_{23} are increased simultaneously until the system reaches the point Q. For this pulse the same condition holds as for the readout pulse: It should be fast enough to not allow for spin-flip transitions into the lower-lying states with $S_z = 1,2$ [45].

Decoherence. The main source of decoherence in GaAs-based spin qubits is known to be the fluctuating bath of nuclear spins that couples to the qubit states through a hyperfine interaction [1,6,23]. The effect of the ensemble of $\sim 10^6$ nuclear spins in each quantum dot can, to good approximation, be modeled as a randomly and slowly fluctuating effective magnetic field $\mathbf{K}_i$ acting on the electrons localized in the dot i. The fluctuations are slow enough that the field can be considered as static on the time scale of a single qubit operation, but it varies randomly over the course of many measurement cycles. The rms value of these random fields was reported to be $K = 1$–3 mT in typical GaAs quantum dots [3,23,52]. The resulting uncertainty in the qubit level splitting translates to a decoherence time T_2^* of tens of ns, and forms at present the bottleneck for further improvement of the performance of GaAs-based spin qubits.

To understand the effect of hyperfine interaction on the singlet-only qubit, we write the effective Hamiltonian

$$\hat{H}_{\rm hf} = \frac{g\mu_{\rm B}}{2}\sum_{i,\alpha,\beta}\hat{c}^\dagger_{i,\alpha}\mathbf{K}_i\cdot\boldsymbol{\sigma}_{\alpha\beta}\hat{c}_{i,\beta}, \tag{6}$$

and project this Hamiltonian to the qubit subspace,

$$\hat{H}_{\rm hf,qb} = 0. \tag{7}$$

This confirms that, to leading order, the nuclear fields do not affect the qubit and thus do not cause any decoherence. The hyperfine Hamiltonian does, however, couple both qubit states to all nine four-electron triplet states. Coupling to the triplet states with $S_z = \pm 1$ is mediated by K_i^x and K_i^y, but transitions to these states are strongly suppressed by the large Zeeman energy E_Z. The z components of the nuclear fields couple $|0\rangle$ and $|1\rangle$ to $|T_{1,2,3}\rangle$, and this coupling (i) can cause leakage out of the qubit space, analogous to leakage to the spin-$\frac{1}{2}$ quadruplet state in the triple-dot XO qubit, and (ii) can yield a higher-order shift in the qubit splitting, contributing to qubit decoherence. Both effects are suppressed by the small factor $g\mu_{\rm B}K/J$ (where J is the typical energy scale of the exchange energies J_{ij}), and the decoherence time resulting from the fluctuations of the qubit splitting [53] can be estimated as $T_2^* \sim \hbar J/(g\mu_{\rm B}K)^2$. For typical parameters ($J = 2$ μeV and $K = 1$ mT) this would present an improvement of two orders of magnitude over other GaAs-based spin qubits, where $T_2^* \sim \hbar/g\mu_{\rm B}K$.

To support these claims, we perform numerical simulations of resonant driving of the qubit. We project the Hamiltonian (1) to the 12-dimensional subspace of all (1,1,1,1), (2,0,1,1), (1,0,2,1), and (1,0,1,2) states with $S_z = 0$. We diagonalize the resulting Hamiltonian at the point Q [see Fig. 1(b)] using the same parameters as before and specifying $t = 16$ μeV; this yields all eigenstates at $\epsilon_{14} = 0$ as well as the qubit splitting $\hbar\omega_0$. We initialize in the lowest-lying singlet state $|0\rangle$, and then let the system evolve under the Hamiltonian $\hat{H} + \hat{H}_{\rm hf}$ where we include resonant driving $\epsilon_{14} = A\cos(\omega_0\tau)$ and four random nuclear fields $\mathbf{K}_i$. In Fig. 2 (solid blue) we show the resulting time-dependent probability to find the system in $|1\rangle$, where we used $A = 2.5$ μeV and averaged over 2500 random nuclear field configurations with the $g\mu_{\rm B}K_i^{x,y,z}$ drawn from a normal distribution with mean zero and $\sigma = 0.07$ μeV. We observe eight Rabi oscillations in $\sim$450 ns without any significant decay [54]. Of course, at longer

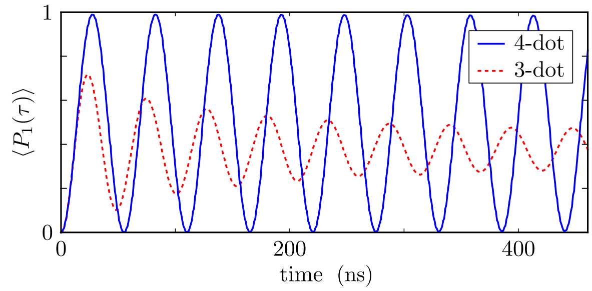

FIG. 2. Solid blue: Calculated time-dependent expectation value of $|1\rangle\langle 1|$ after initializing in $|0\rangle$ and driving resonantly with $\epsilon_{14} \propto \cos(\omega_0\tau)$, averaged over 2500 random configurations of the nuclear fields. Dashed red: Equivalent result for the triple-dot XO setup, using the same parameters.

times eventually leakage out of the qubit space as well as higher-order corrections due to the nuclear fields will suppress the oscillations in $\langle P_1(\tau)\rangle$.

As a comparison, we also performed equivalent simulations of resonant driving of a triple-dot XO qubit (cf. Ref. [23]), using exactly the same parameters (basically setting $t_{23} = 0$ and adjusting ω_0 to the new qubit splitting). The result is plotted with a red dashed line in Fig. 2; in this case the hyperfine-induced decay of $\langle P_1(\tau)\rangle$ is already significant in the first few Rabi periods. The clear contrast between the two curves illustrates the improvement presented by our quadruple-dot XO qubit.

Relaxation. Electron-phonon coupling can contribute to qubit relaxation, i.e., induce dissipative transitions from $|1\rangle$ to $|0\rangle$. The associated relaxation rate can be estimated using Fermi's golden rule, $\Gamma_{\rm rel} = \frac{2\pi}{\hbar}\sum_f |\langle f|\hat{H}_{\text{e-ph}}|i\rangle|^2\delta(E_f - E_i)$, where the initial state is $|1\rangle|\text{vac}\rangle$ (with $|\text{vac}\rangle$ denoting the phonon vacuum) and the sum runs over all possible final states $|0\rangle|1_{\mathbf{k},p}\rangle$ where one phonon has been created with wave vector $\mathbf{k}$ and polarization p. We use an electron-phonon Hamiltonian

$$\hat{H}_{\text{e-ph}} = \sum_{\mathbf{k},p} \lambda_{\mathbf{k},p}\hat{\rho}_{\mathbf{k}}(\hat{a}_{\mathbf{k},p} + \hat{a}^\dagger_{-\mathbf{k},p}), \tag{8}$$

where $\hat{a}^\dagger_{\mathbf{k},p}$ creates a phonon in mode $\{\mathbf{k},p\}$, $\hat{\rho}_{\mathbf{k}}$ is the Fourier transform of the electronic density matrix, and $\lambda_{\mathbf{k},p}$ are the coupling parameters (see, e.g., Ref. [55]). At typical qubit splittings the coupling to piezoelectric phonons dominates, in which case an explicit evaluation of $\Gamma_{\rm rel}$ yields to leading order in t/Δ the estimate [45]

$$\Gamma_{\rm rel} \approx \frac{t^4}{\Delta^4}\frac{\omega_0^3 d^3}{v^3}\frac{(eh_{14})^2}{10\pi\hbar\rho v^2 d}, \tag{9}$$

where v is the phonon velocity (for convenience now assumed equal for all three polarizations), d the distance between neighboring dots, h_{14} the piezoelectric constant, and ρ denotes the mass density of the semiconductor (for GaAs, $v \sim 4000$ m/s, $h_{14} \approx 1.45 \times 10^9$ V/m, and $\rho \approx 5300$ kg/m^3; see Ref. [56]). Setting $d = 100$ nm, this yields $\Gamma_{\rm rel} = \omega_0^3(t/\Delta)^4(3\times 10^{-23}\ \text{Hz}^{-2})$, which for $\Delta = 5t$ and $\hbar\omega_0 = 1.5\ \mu$eV gives $\Gamma_{\rm rel} = 0.57$ kHz.

Relaxation processes to $|T_3\rangle$ require a change of the spin state of the electrons [57] and are estimated to be smaller by a factor $\sim(g\mu_B K/J)^2$. Dissipative transitions to the lower-lying states with $S_z = 1,2$ require a spin flip and are suppressed by the large Zeeman energy E_Z.

Conclusions. We propose a quantum-dot-based singlet-only spin qubit which is to leading order intrinsically insensitive to randomly fluctuating nuclear fields. Our proposal thus removes the main obstacle for further improvement of spin qubits hosted in semiconductors with spinful nuclei, such as GaAs. Its scalability, full electrical control, and large coherence time make the singlet-only spin qubit one of unprecedented quality.

Acknowledgment. We thank M. S. Rudner for several very helpful discussions.

[1] R. Hanson, L. P. Kouwenhoven, J. R. Petta, S. Tarucha, and L. M. K. Vandersypen, Rev. Mod. Phys. **79**, 1217 (2007).
[2] D. Loss and D. P. DiVincenzo, Phys. Rev. A **57**, 120 (1998).
[3] F. H. L. Koppens, C. Buizert, K. J. Tielrooij, I. T. Vink, K. C. Nowack, T. Meunier, L. P. Kouwenhoven, and L. M. K. Vandersypen, Nature (London) **442**, 766 (2006).
[4] J. M. Elzerman, R. Hanson, L. H. Willems van Beveren, B. Witkamp, L. M. K. Vandersypen, and L. P. Kouwenhoven, Nature (London) **430**, 431 (2004).
[5] S. I. Erlingsson and Y. V. Nazarov, Phys. Rev. B **66**, 155327 (2002).
[6] I. A. Merkulov, A. L. Efros, and M. Rosen, Phys. Rev. B **65**, 205309 (2002).
[7] A. V. Khaetskii, D. Loss, and L. Glazman, Phys. Rev. Lett. **88**, 186802 (2002).
[8] V. N. Golovach, M. Borhani, and D. Loss, Phys. Rev. B **74**, 165319 (2006).
[9] C. Flindt, A. S. Sørensen, and K. Flensberg, Phys. Rev. Lett. **97**, 240501 (2006).
[10] S. Nadj-Perge, S. M. Frolov, E. P. A. M. Bakkers, and L. P. Kouwenhoven, Nature (London) **468**, 1084 (2010).
[11] A. V. Khaetskii and Y. V. Nazarov, Phys. Rev. B **64**, 125316 (2001).
[12] J. Danon and Y. V. Nazarov, Phys. Rev. B **80**, 041301(R) (2009).
[13] D. P. DiVincenzo, D. Bacon, J. Kempe, G. Burkard, and K. B. Whaley, Nature (London) **408**, 339 (2000).
[14] J. R. Petta, A. C. Johnson, J. M. Taylor, E. A. Laird, A. Yacoby, M. D. Lukin, C. M. Marcus, M. P. Hanson, and A. C. Gossard, Science **309**, 2180 (2005).
[15] J. M. Taylor, J. R. Petta, A. C. Johnson, A. Yacoby, C. M. Marcus, and M. D. Lukin, Phys. Rev. B **76**, 035315 (2007).
[16] J. Medford, J. Beil, J. M. Taylor, S. D. Bartlett, A. C. Doherty, E. I. Rashba, D. P. DiVincenzo, H. Lu, A. C. Gossard, and C. M. Marcus, Nat. Nanotechnol. **8**, 654 (2013).
[17] E. A. Laird, J. M. Taylor, D. P. DiVincenzo, C. M. Marcus, M. P. Hanson, and A. C. Gossard, Phys. Rev. B **82**, 075403 (2010).
[18] M. Russ and G. Burkard, arXiv:1611.09106.

[19] F. Martins, F. K. Malinowski, P. D. Nissen, E. Barnes, S. Fallahi, G. C. Gardner, M. J. Manfra, C. M. Marcus, and F. Kuemmeth, Phys. Rev. Lett. **116**, 116801 (2016).
[20] M. D. Reed, B. M. Maune, R. W. Andrews, M. G. Borselli, K. Eng, M. P. Jura, A. A. Kiselev, T. D. Ladd, S. T. Merkel, I. Milosavljevic, E. J. Pritchett, M. T. Rakher, R. S. Ross, A. E. Schmitz, A. Smith, J. A. Wright, M. F. Gyure, and A. T. Hunter, Phys. Rev. Lett. **116**, 110402 (2016).
[21] Y.-P. Shim and C. Tahan, Phys. Rev. B **93**, 121410(R) (2016).
[22] W. A. Coish and D. Loss, Phys. Rev. B **72**, 125337 (2005).
[23] J. Medford, J. Beil, J. M. Taylor, E. I. Rashba, H. Lu, A. C. Gossard, and C. M. Marcus, Phys. Rev. Lett. **111**, 050501 (2013).
[24] S. Mehl and D. P. DiVincenzo, Phys. Rev. B **87**, 195309 (2013).
[25] J.-T. Hung, J. Fei, M. Friesen, and X. Hu, Phys. Rev. B **90**, 045308 (2014).
[26] M. S. Rudner and L. S. Levitov, Phys. Rev. Lett. **99**, 036602 (2007).
[27] I. T. Vink, K. C. Nowack, F. H. L. Koppens, J. Danon, Y. V. Nazarov, and L. M. K. Vandersypen, Nat. Phys. **5**, 764 (2009).
[28] M. S. Rudner, L. M. K. Vandersypen, V. Vuletić, and L. S. Levitov, Phys. Rev. Lett. **107**, 206806 (2011).
[29] S. M. Frolov, J. Danon, S. Nadj-Perge, K. Zuo, J. W. W. van Tilburg, V. S. Pribiag, J. W. G. van den Berg, E. P. A. M. Bakkers, and L. P. Kouwenhoven, Phys. Rev. Lett. **109**, 236805 (2012).
[30] H. Bluhm, S. Foletti, D. Mahalu, V. Umansky, and A. Yacoby, Phys. Rev. Lett. **105**, 216803 (2010).
[31] H. Bluhm, S. Foletti, I. Neder, M. Rudner, D. Mahalu, V. Umansky, and A. Yacoby, Nat. Phys. **7**, 109 (2011).
[32] F. K. Malinowski, F. Martins, P. D. Nissen, E. Barnes, Ł. Cywiński, M. S. Rudner, S. Fallahi, G. C. Gardner, M. J. Manfra, C. M. Marcus, and F. Kuemmeth, Nat. Nanotechnol. **12**, 16 (2016).
[33] N. Rohling and G. Burkard, Phys. Rev. B **93**, 205434 (2016).
[34] M. D. Shulman, S. P. Harvey, J. M. Nichol, S. D. Bartlett, A. C. Doherty, V. Umansky, and A. Yacoby, Nat. Commun. **5**, 5156 (2014).
[35] F. A. Zwanenburg, A. S. Dzurak, A. Morello, M. Y. Simmons, L. C. L. Hollenberg, G. Klimeck, S. Rogge, S. N. Coppersmith, and M. A. Eriksson, Rev. Mod. Phys. **85**, 961 (2013).
[36] K. Eng, T. D. Ladd, A. Smith, M. G. Borselli, A. A. Kiselev, B. H. Fong, K. S. Holabird, T. M. Hazard, B. Huang, P. W. Deelman, I. Milosavljevic, A. E. Schmitz, R. S. Ross, M. F. Gyure, and A. T. Hunter, Sci. Adv. **1**, e1500214 (2015).
[37] M. Veldhorst, J. C. C. Hwang, C. H. Yang, A. W. Leenstra, B. de Ronde, J. P. Dehollain, J. T. Muhonen, F. E. Hudson, K. M. Itoh, A. Morello, and A. S. Dzurak, Nat. Nanotechnol. **9**, 981 (2014).
[38] D. Bacon, J. Kempe, D. A. Lidar, and K. B. Whaley, Phys. Rev. Lett. **85**, 1758 (2000).
[39] D. A. Lidar and K. B. Whaley, in *Irreversible Quantum Dynamics*, edited by F. Benatti and R. Floreanini (Springer, Berlin, 2003), pp. 83–120.
[40] V. W. Scarola, K. Park, and S. Das Sarma, Phys. Rev. Lett. **93**, 120503 (2004).
[41] B. Antonio and S. Bose, Phys. Rev. A **88**, 042306 (2013).
[42] In fact, if sensitive enough, one charge sensor could suffice, as long as it is not placed equidistant from any pair of dots.
[43] G. Burkard, D. Loss, and D. P. DiVincenzo, Phys. Rev. B **59**, 2070 (1999).
[44] J. M. Taylor, V. Srinivasa, and J. Medford, Phys. Rev. Lett. **111**, 050502 (2013).
[45] See Supplemental Material at http://link.aps.org/supplemental/10.1103/PhysRevB.95.241303 for more detailed discussions and derivations of the equations presented in the main text, which includes Refs. [46–51].
[46] J. R. Schrieffer and P. A. Wolff, Phys. Rev. **149**, 491 (1966).
[47] J. Danon, Phys. Rev. B **88**, 075306 (2013).
[48] R. Thalineau, S. Hermelin, A. D. Wieck, C. Bäuerle, L. Saminadayar, and T. Meunier, Appl. Phys. Lett. **101**, 103102 (2012).
[49] T. Takakura, A. Noiri, T. Obata, T. Otsuka, J. Yoneda, K. Yoshida, and S. Tarucha, Appl. Phys. Lett. **104**, 113109 (2014).
[50] M. R. Delbecq, T. Nakajima, T. Otsuka, S. Amaha, J. D. Watson, M. J. Manfra, and S. Tarucha, Appl. Phys. Lett. **104**, 183111 (2014).
[51] D. M. Zajac, T. M. Hazard, X. Mi, E. Nielsen, and J. R. Petta, Phys. Rev. Appl. **6**, 054013 (2016).
[52] A. C. Johnson, J. R. Petta, J. M. Taylor, A. Yacoby, M. D. Lukin, C. M. Marcus, M. P. Hanson, and A. C. Gossard, Nature (London) **435**, 925 (2005).
[53] $K_i^{x,y}$ can cause a similar higher-order shift in the qubit splitting, but the resulting contribution to the dephasing rate $1/T_2^*$ is smaller by a factor J/E_Z .
[54] We note that these simulations include hyperfine-induced leakage out of the qubit space to other states with $S_z = 0$.
[55] P. Stano and J. Fabian, Phys. Rev. B **74**, 045320 (2006).
[56] O. Madelung, *Semiconductors: Data Handbook*, 3rd ed. (Springer, Berlin, 2004).
[57] Possible contributions from spin-orbit interaction to relaxation to $|T_3\rangle$ could be suppressed by applying the external magnetic field perpendicularly to the qubit plane.